Reuse of ammonium sulfate double salt crystals formed during electrolytic manganese production

Shaobo Zhang, Sanfan Wang, Qianqian Zhang, Yanhong Li, Yue Xing and Guangyi Ren

ABSTRACT

Ammonium sulfate double salt crystals (ASDSCs) are formed during the electrolytic production of manganese. Typically, the large volume of ASDSCs accumulates in the open air, and this leads to serious environmental pollution and wastage of resources. In this study, we developed a new double-membrane three-chamber electrolysis method. In this method, ASDSCs were dissolved in water and then pretreated stepwise to precipitate manganese(II) carbonate and magnesium carbonate. These precipitates were filtered and the filtrate (mainly ammonium sulfate) was subjected to double-membrane three-chamber electrodecomposition to produce sulfuric acid and ammonia. Further investigations showed that under the optimal conditions of current density of 250 A/m^2, electrolysis time of 18 h, and temperature of 40 °C, the decomposition rate of ammonium sulfate reached as high as 96.15%. Thus, using this method, ASDSCs can be completely decomposed, which resolves the problem of environmental pollution and provides certain economic benefits to enterprises.

Key words | ammonium sulfate double salt crystals, double-membrane three-chamber, ion exchange membrane electrolyzer, ion transport, recycling

Shaobo Zhang
Sanfan Wang (corresponding author)
Qianqian Zhang
Yanhong Li
Yue Xing
Guangyi Ren
School of Environmental and Municipal Engineering,
Lanzhou Jiaotong University,
Lanzhou 730070,
China
E-mail: *sfwang1612@163.com*

Shaobo Zhang
Sanfan Wang
Qianqian Zhang
Yanhong Li
Guangyi Ren
Engineering Research Center of Ministry of Education for Comprehensive Utilization of Water Resources in Cold and Drought Areas,
Lanzhou 730070,
China

HIGHLIGHTS

- No waste residue and liquid will be generated in the treatment process.
- Can solve the environmental problems caused by ammonium sulfate double salt crystal accumulation.
- Two-membrane three-chamber electrolysis method is used for further treatment.
- Ammonium sulfate in the middle compartment is decomposed into sulfuric acid and ammonia water.
- The manganese(II) carbonate filtered by impurity removal can be directly sold as a commodity.

doi: 10.2166/wst.2020.374

GRAPHICAL ABSTRACT

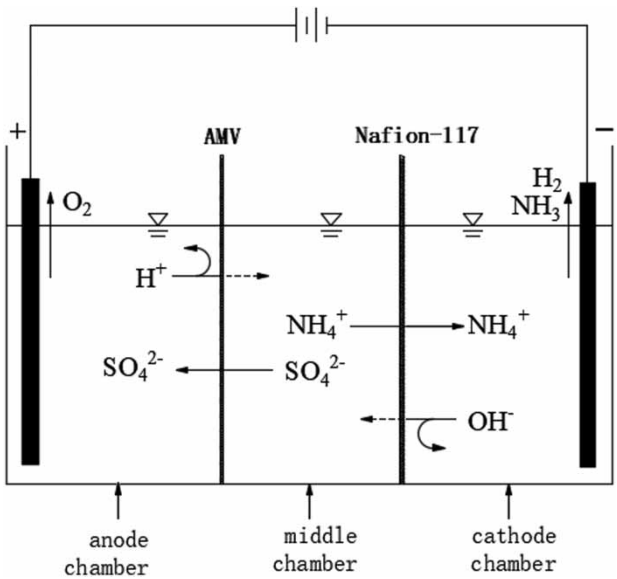

INTRODUCTION

The current annual production capacity of electrolytic manganese in China is ~1.88 million tons, which accounts for ~98% of the global production (Zhou 2010). It is estimated that the global demand for manganese will increase by 83% by 2021 (Lu *et al.* 2014). Concurrent to such rapid development of the electrolytic manganese metal industry, it is expected that the waste slag generated during production will have a great impact on the environment. Various types of waste slag are generated in this process, namely, manganese slag, fine filter slag, ammonium sulfate double salt crystals (ASDSCs), and anode slag (Zhang *et al.* 2016). It is worth noting that the addition of sulfuric acid (H_2SO_4) to the manganese ore also results in the leaching of Mg^{2+} together with Mn^{2+}. Consequently, because the electrolytic manganese anode solution is used in a closed cycle, Mg^{2+} concentration in the manganese anode solution increases by ~2 g/L each cycle. According to the same ion effect, the solubility of manganese sulfate and ammonium sulfate in the electrolyte decreases, leading to their precipitation in the form of ammonium sulfate manganese and ammonium sulfate magnesium double salt crystals (Jia *et al.* 2018). According to statistics of relevant electrolytic manganese enterprises, 0.8–2.5 tons of ASDSCs are produced for every 1 ton electrolytic manganese metal (Method 2011). ASDSCs are a powdery substance with fine white particles and good water retention. The moisture content of fresh ammonium sulfate slag is determined to be as high as 49.73–51.97%. Inductively coupled plasma (ICP) detection of ASDSCs have revealed that the main substance in ASDSC is ammonium sulfate, and they also contain Mn, Mg, and trace amounts of Ca, Fe, Zn, etc.

Presently, there are many treatment methods for the different types of slag other than ASDSCs, including making cement (Feng *et al.* 2006; Zhou *et al.* 2013), bricks (Yang *et al.* 2014; Zhou *et al.* 2014), and ceramic materials (Ye *et al.* 2018), recovering extracted manganese (Shu *et al.* 2016a; Li *et al.* 2008), as synthetic zeolites (Li *et al.* 2015a, 2015b), solidifying landfill (Shu *et al.* 2016b; Shu *et al.* 2018), etc. To the best of our knowledge, to date, there are only three patents reporting on the treatment of ASDSCs. It has been reported that the ASDSCs can be mixed with the anode slag for roasting, followed by the addition of water for filtration and electrolysis of the filtrate to recover manganese (Tao *et al.* 2018). In another method, ammonium persulfate and oxalic acid dihydrate have been added for fractional precipitation (He *et al.* 2011). Furthermore, researchers have introduced carbon dioxide gas into the aqueous solution of ASDSCs to generate manganese(II) carbonate precipitate, which is filtered off. The filtrate is then

reacted with magnesium oxide to generate magnesium sulfate and aqueous ammonia (Jia *et al.* 2018). However, the above-mentioned methods have disadvantages such as high energy consumption and high cost, in addition to being complex processes whereby the products generated after treatment cannot be directly utilized and need further treatment, which prevents their application to actual industrial production. A large volume of ASDSCs piles up in the open air, and NH_4^+ and Mn^{2+} in the crystals dissolve out under the scouring of rainwater and reach groundwater through soil. Excessive ammonium leads to eutrophication. Although manganese is an essential element of the human body, excessive intake causes serious damage to the central nervous system, cardiovascular system, and urinary system. How to recycle the increasing ASDSCs has become an urgent problem for manganese-related enterprises and local governments (Wang *et al.* 2012). In order to solve the above problems and further recycle ASDSCs, this paper proposes a double-membrane three-chamber electrolysis method, which recycles ASDSCs into manganese carbonate, magnesium carbonate, sulfuric acid, and ammonia water for recycling production, thus realizing the purpose of recycling ASDSCs.

EXPERIMENTAL

Materials and reagents

The anolyte and catholyte of the electrolytic cell were sulfuric acid solution and aqueous ammonia solution, respectively. The solution in the middle compartment of the electrolytic cell was the filtrate obtained after the ASDSC was dissolved in water. The chemical reagents used in the experiments were of analytical grade and all solutions were prepared with deionized water with a resistivity greater than 18 MΩ cm. Fresh ASDSCs were taken from Tianyuan Manganese Industry Group in Ningxia. The ICP analysis results of the ASDSCs are summarized in Table 1. The parameters of experimental membranes are given in Table 2 and the standard water quality parameters of the solution after pretreatment are given in Table 3.

The electrolytic cell had dimensions of $0.22 \times 0.22 \times 0.105\ m^3$ and was made of epoxy resin. The electrolytic cell had a double-membrane three-chamber structure. An anion exchange membrane and a cation exchange membrane were utilized to sequentially divide the unit electrolytic cell into a cathode chamber, a middle chamber, and an anode chamber. The effective volume of each compartment was 650 mL. The effective membrane size of the ion exchange membrane was $0.16 \times 0.16\ m^2$. The anode is a $0.01147\ m^2$ ($0.14 \times 0.105\ m^2$) titanium-based iridium ruthenium electrode plate. The cathode plate was a Stainless Steel 316 Electrode of same area and fixed at a distance of 0.075 m from the anode plate. A DC power supply (Shenzhen Mestek Electronics Co., Ltd, China) was used, and the current and voltage ranges were 0–5 A and 0–32 V, respectively.

Experimental principle

The implementation of the double-membrane three-chamber electrolysis process mainly depends on the selective permeability of the anion and cation exchange membranes. This technology is a membrane application

Table 1 | Results of ICP analysis of ASDSCs

Sampling location	Zn (%)	Fe (%)	Mg (%)	Ca (%)	Mn (g/L)	$(NH_4)_2SO_4$ (g/L)
Transfer tank	0.016	0.088	6.67	0.061	5.64	36.71
High pool	0.013	0.063	6.78	0.054	6.01	36.18
Neutral liquid pool	0.0055	0.051	2.55	0.015	1.98	37.46
Neutral flow cell	0.013	0.054	6.53	0.052	3.08	37.12

Table 3 | Standard water quality parameters of the solution after pretreatment

Turbidity (NTU)	Conductivity (μs/cm)	pH	Density (g/cm^3)
6.7	22,792	8.12	1.1276

Table 2 | Performance indicators of the experimental membranes (Zhou *et al.* 2016)

Membrane type	Functional group	Exchange capacity (mmol/l)	Resistance (Ω/cm^2)	Permselectivity (%)	Strength (kPa)	Thickness (μm)
Ionsep-HCC	RSO_3H	2.3	2.5	>95	600	600
Selemion-HSF	RSO_3H	2.4	1.9	>97	200	150
Nafion-117	RSO_3H	1.1	1.5	>98	320	183
AMV	RN $(CH_3)_3Cl$	2.0	2.5	>96	200	120

process with DC electric field gradient as the main driving force. Besides the electric field gradient, electrolysis is also affected by the concentration and temperature (Sata 2000; Tanaka 2003). Under the influence of these factors, the transport of ions in the electrolytic cell involves ion migration, water molecule electro-osmosis, ion diffusion, etc. The possible ion transport processes in the double-membrane three-chamber electrolytic cell are shown in Figure 1. In the cathode chamber, water is electrolyzed into H_2, and OH^- ions are generated at the same time. As the NH_4^+ concentration in the middle chamber is several orders of magnitude higher than that of H^+, the charge balance across the membrane is mainly maintained by NH_4^+. The NH_4^+ ions are attracted to the cathode and move out of the middle chamber through the anode membrane into the cathode chamber. The OH^- ions generated in the cathode chamber is blocked by the anode membrane, and combine with NH_4^+ ions passing through the anode membrane to produce ammonia water. The concentration of ammonia water gradually increases and excess ammonia gas can be extracted through negative pressure. The water present in the anode chamber is electrolyzed to produce H^+ and O_2, and SO_4^{2-} ions move through the negative membrane into the anode chamber. Eventually, H^+ and SO_4^{2-} accumulate in the anode chamber, and the concentration of sulfuric acid increases considerably. These above-mentioned electrochemical reactions are shown in Equations (1)–(4).

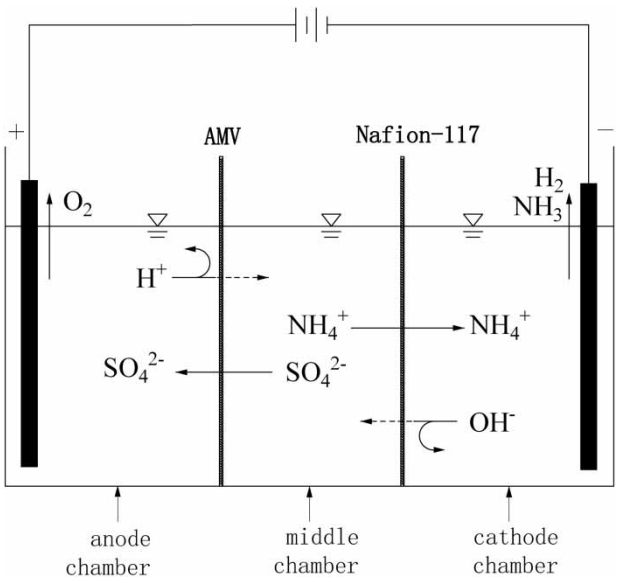

Figure 1 | Schematic diagram of ion transport in the electrolytic cell.

Cathode chamber:

$$2H_2O + 2e^- \rightarrow H_2 \uparrow + 2OH^- \quad (1)$$

$$NH_4^+ + OH^- \rightarrow NH_3 \cdot H_2O \quad (2)$$

Middle chamber:

$$(NH_4)_2SO_4 \rightarrow 2NH_4^+ + SO_4^{2-} \quad (3)$$

Anode chamber:

$$2H_2O - 2e^- \rightarrow 2H^+ + O_2 \uparrow \quad (4)$$

Experimental operation

Electrolytic manganese enterprises hope to fully recover the Mn^{2+} in ASDSCs. Therefore, the first step is to separate the Mn^{2+} so that it can be directly used in the production of electrolytic manganese. ASDSCs contain a large volume of Mg^{2+}. If not removed, a large amount of magnesium hydroxide flocculent precipitate will be formed in the cathode chamber, hindering electrolysis. This necessitates pretreatment of the solution before electrolysis. The ASDSCs can be completely dissolved in water, and the impurity removal effect has a great influence on the subsequent electrolysis and product purity. If Mn^{2+} is not completely removed, a small amount of Mn^{2+} in the middle compartment passes through the anode membrane into the cathode compartment. Under these conditions, the small amount of Mn^{2+} will not generate the manganese(II) hydroxide precipitate, but will instead gain electrons and attach to the cathode plate in the form of metallic manganese. If Mg^{2+} is not completely removed, it passes through the anode membrane and enters the cathode chamber to react with the hydroxyl ions. This produces magnesium hydroxide, reduces the decomposition rate of ammonium sulfate in the intermediate compartment, affects the purity of ammonia water, and may also block the circulation pipeline in future on-site production. In addition, the magnesium hydroxide precipitates adhere to the cation exchange membrane, increasing its resistance. ASDSCs were dissolved in deionized water (1:2 ratio) at ambient temperature. The solution was filtered and ammonia water was added to adjust the pH to 7.5. Next, 22 g of ammonium bicarbonate were added per liter of the solution, which was stirred for 20 min to generate manganese carbonate precipitate. The precipitate was removed by vacuum filtration and ammonia water was added to the filtrate to

adjust the pH to 9.5. Subsequently, 90 g of ammonium bicarbonate was added per liter of the solution and stirred for an additional 20 min to generate the magnesium carbonate precipitate. This precipitate was also removed by suction filtration. The order of adding electrolytes into the electrolytic cell was as follows: 0.05 mol/L sulfuric acid solution was injected into the anode chamber, followed by 0.05 mol/L ammonia into the cathode chamber, and finally the filtered liquid was injected into the middle chamber. The electrolyzer was assembled with a water-bath to heat and control the reaction temperature, and a direct current power supply was used for electrolysis. To study the influence of various experimental conditions on electrolysis, experiments were carried out using different membranes, varying the reaction time, current density, reaction temperature, and initial concentrations of acid and alkali in the compartments on both sides. Samples were withdrawn from three compartments every hour, and each compartment took three samples from the same location to obtain the average value. After the experiment, the electrolyzer and membrane were washed with deionized water for the next group of experiments.

Analysis method

The concentration of ammonium sulfate in the middle compartment was determined by the formaldehyde method, and the acid and alkali concentrations were measured by acid–base neutralization titration. Three samples were taken at each time point to calculate the average value. The main components in the ASDSC were measured using ICP, and the slag filtered at each step was analyzed using X-ray diffraction (XRD). Ammonium sulfate decomposition rate $= 1 - \frac{c1 \times V}{c2 \times V}$ where c1 is the initial ammonium sulfate concentration, c2 is the ammonium sulfate concentration after electrolysis for a period of time, and V refers to the volume of the liquid in the middle compartment.

RESULTS AND DISCUSSION

Effect of different types of anode membranes

AMV was used as the anion membrane, and Ionsep-HCC, Selemion-HSF, Nafion-117 were used as different cation membranes. The membrane electrolyzer was operated at a constant temperature of 30 °C and current density of 200 A/m^2, and the results obtained are shown in Figure 2. With an increase in the electrolysis time, the concentration of ammonium sulfate decreased continuously, and the downward trend of the three membranes was similar. NH_4^+ and SO_4^{2-} in the middle compartment moved to the cathode and anode compartments through the anode and cathode membranes, respectively, and

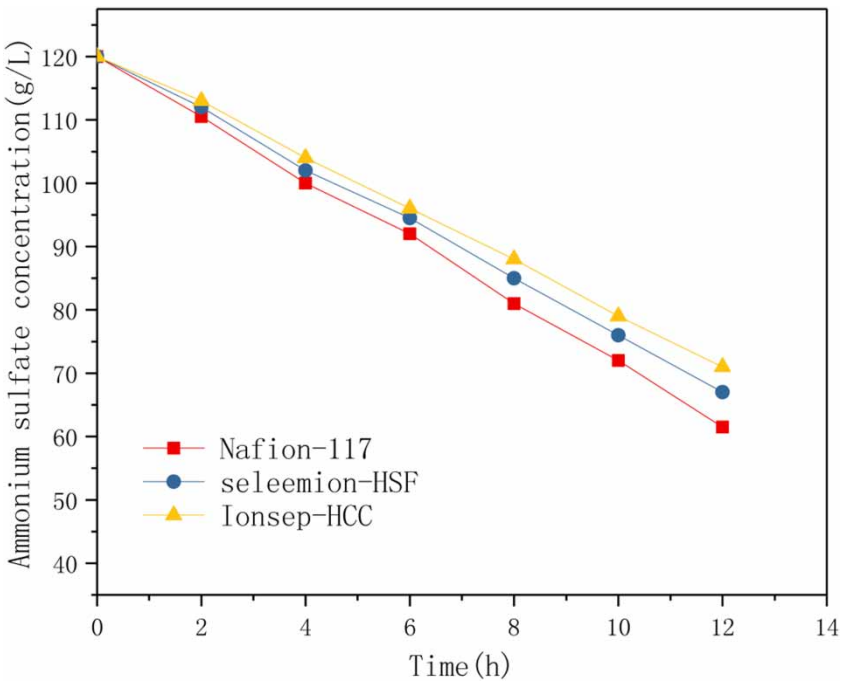

Figure 2 | Effect of different membranes on the decomposition rate of ammonium sulfate (current density 200 A/m^2, 0.05 mol/L H_2SO_4, 0.05 mol/L NH_3·H_2O, T = 30 °C).

the decomposition concentration of ammonium sulfate in the middle compartment decreased continuously. The membrane decomposition effect of Nafion-117 was slightly better than that of the other two membranes. The transport of ions through the ion exchange membrane is based on the Donnan rejection mechanism. The conduction of current in the ion exchange membrane involved the conduction of ions opposite to the fixed charge. The decomposition rate of ammonium sulfate in the middle compartment was highest when the Nafion-117 membrane was installed, probably due to the highest permeability of Nafion-117 among the three membranes. Therefore, AMV and Nafion-117 are used in the subsequent experiments.

Effect of initial acid and alkali concentrations in the two-sided compartments

The effect of different initial acid and alkali concentrations in the two-sided compartments on the ammonium sulfate decomposition rate is shown in Figure 3. Stable voltage corresponding to the initial concentration of compartments on both sides is shown in Table 4. The decreasing ammonium sulfate decomposition rate in the middle compartment was similar at the different acid and alkali concentrations, indicating that the concentration had no obvious effect on the ammonium sulfate decomposition rate. When the concentration of the solution was low, the conductivity of the solution was poor and resistance was slightly high. The electrochemical impedance analysis (EIS) test results of Zhang *et al.* (2017) showed that the electrostatic force between the fixed groups and counter ions in the membrane was very strong when the concentration of the solution was low. This condition limits the movement of ions through the membrane and the membrane resistance is large. A higher concentration of the solution implies higher conductivity and lower resistance. In addition, a high concentration has a shielding effect on the electrostatic force, which enhances the conductivity of the ion exchange membrane. It also reduces the thickness of the boundary layer of the ion exchange membrane and the membrane resistance. Consequently, the resistance of the entire system and working voltage decreases. During electrolysis, the change in concentration of the compartments on both sides had no effect on the electric decomposition rate, but did affect the magnitude of the operating voltage.

Table 4 | Stable voltage corresponding to initial concentration of compartments on both sides

Concentration (mol/L)	0.05	0.1	0.15	0.2	0.25
Voltage (V)	6.3	6.12	5.87	5.6	5.41

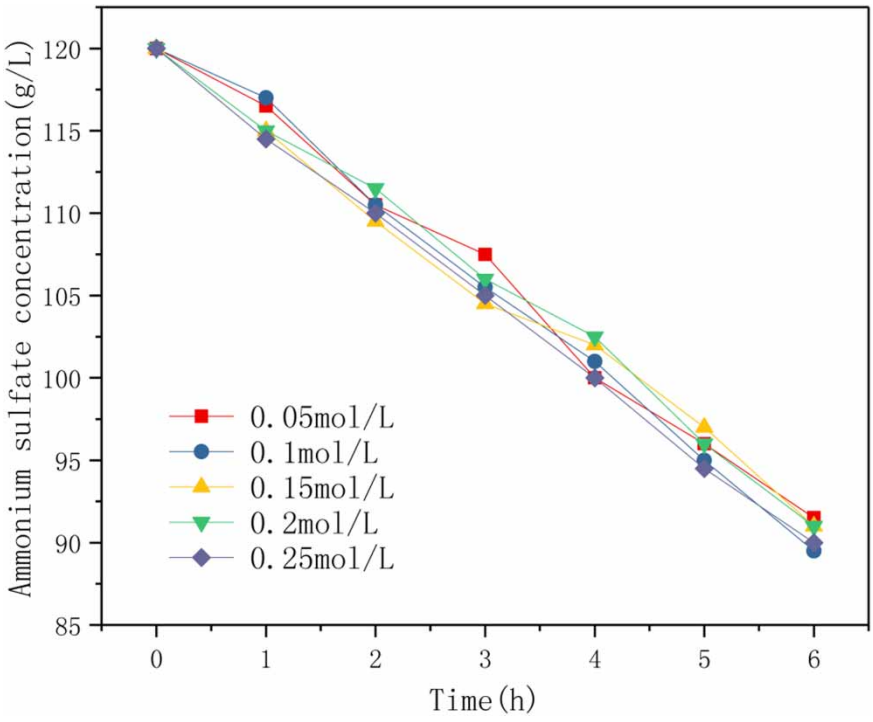

Figure 3 | Effect of initial acid and alkali concentrations in the two-sided compartments on the decomposition rate of ammonium sulfate (current density 200 A/m^2, T = 30 °C).

Effect of temperature on electrolysis

To study the effect of different temperatures on the decomposition rate of ASDSCs, under the condition of current density of 200 A/m^2, the membrane electrolysis experiments were carried out at 30, 35, 40, 45, and 50 °C. Since high temperatures would have an irreversible influence on the structure of the ion exchange membrane and render it useless, the maximum temperature was set as 50 °C. The effect of different temperatures on the decomposition rate of ammonium sulfate in the middle compartment is shown in Figure 4. The decomposition of ammonium sulfate was fastest at 40 °C. The mass transfer process of the ion exchange membrane in solution involved three stages, namely, the migration of ions in the main solution, in the membrane, and in the boundary layer (Park *et al.* 2006). Under the electric field, ions in the solution move directionally toward the two electrodes. However, since the speed of ions in the solution is faster than the speed of ions passing through the membrane, concentration polarization occurs in the boundary layer. Generally, a higher temperature corresponds to a stronger electrostatic force shielding effect between the fixed groups and counter ions in the membrane. Additionally, changes in physical properties, such as swelling degree of the membrane material and the decrease in the Donnan effect caused by the increasing temperature, reduce the thickness of the diffusion boundary layer and the concentration polarization phenomenon. This observation is consistent with the results reported by Zhang *et al.* (2017) through electrochemical impedance spectroscopy analysis. Cheng *et al.* (2010) reported the effect of temperature on the ion migration rate and the electrochemical reaction rate on the electrode surface. The reaction rate on the electrodes of both compartments increased with the increasing temperature, which increased the decomposition rate. However, a high temperature would lead to the decomposition of the functional groups of the anion exchange membrane, increasing the ion leakage rate, and thus slightly decreasing the decomposition rate. The optimal temperature for electrolysis was 40 °C.

Effect of current density

Continuous electrolysis was carried out at a current density of 100, 150, 200, 250 and 300 A/m^2 and a temperature of 40 °C for 6 h. The change in ammonium sulfate concentration in the intermediate compartment with current density is shown in Figure 5. In the range of 100–250 A/m^2, the decomposition rate of ammonium sulfate in the middle compartment increased as the current density

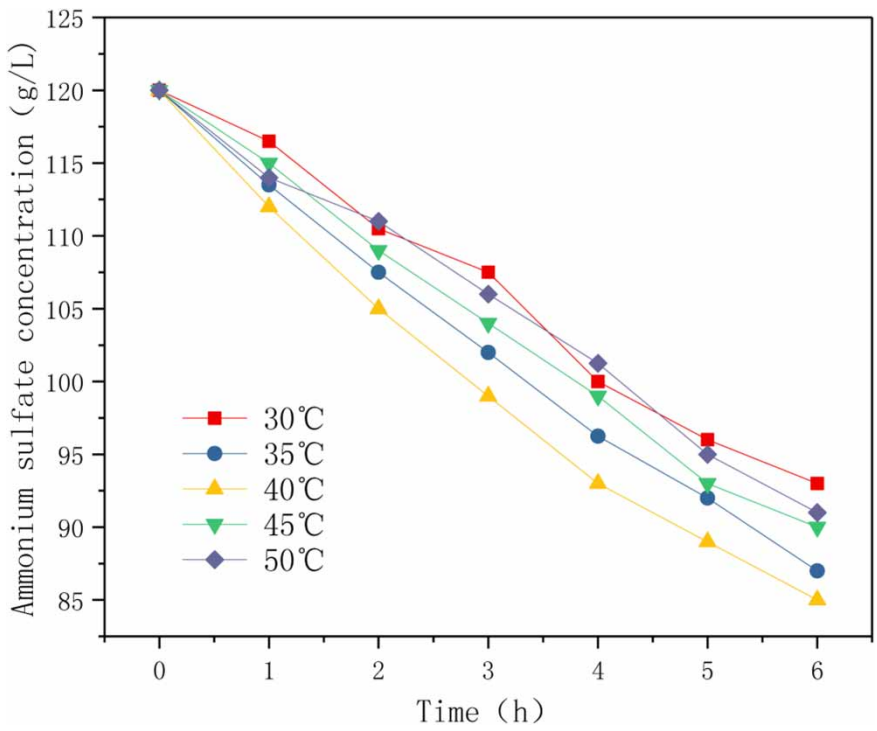

Figure 4 | Effect of temperature on the rate of ammonium sulfate decomposition (current density 200 A/m^2, 0.05 mol/L H_2SO_4, 0.05 mol/L $NH_3{\cdot}H_2O$).

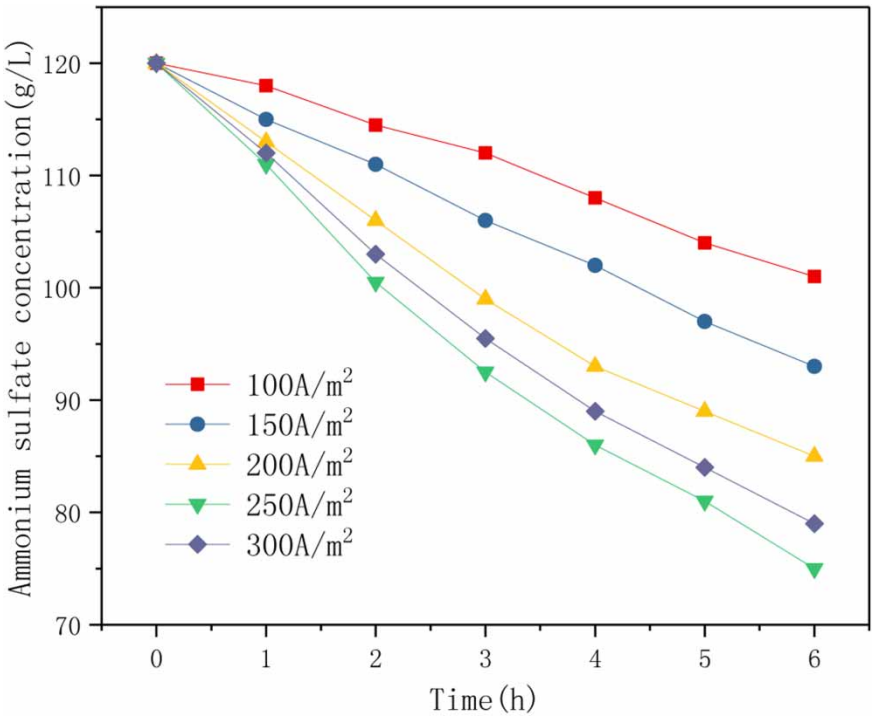

Figure 5 | Effect of current density on the decomposition rate of ammonium sulfate (T = 40 °C, 0.05 mol/L H_2SO_4, 0.05 mol/L $NH_3{\cdot}H_2O$).

was increased. However, the decomposition rate of ammonium sulfate decreased slightly when the current density was 300 A/m^2. Upon increasing current density, which is the driving force of the electrode to the ions in the solution, the penetration rate of NH_4^+ and SO_4^{2-} increased, and the decomposition rate increased. At the current density of 300 A/m^2, the decrease in decomposition rate may be attributed to the fact that the cation exchange membrane was not suitable for such high current density (Shi *et al.* 2019) As the current density further increased to near the limit current density, the ion transport speed in the membrane increased. The ion transport speed in the solution was slower than that in the membrane, resulting in a sharp drop in the ion concentration in the diffusion layer on the membrane surface (i.e., concentration polarization phenomenon). The current density of 300 A/m^2 exceeded the limit current density of the membrane. At this stage, phenomena such as water splitting, membrane discharge, and electric convection may occur (Luo *et al.* 2018). Therefore, the decomposition rate of ammonium sulfate decreases.

Effect of time on electrolysis

The electrolyzer was operated at a constant current density of 250 A/m^2 and a temperature of 40 °C. The decomposition rate of ammonium sulfate in the middle compartment during electrolysis varied with time, as shown in Figure 6. The results showed that the decomposition rate of ammonium sulfate increased linearly with increasing reaction time, and the speed decreased in the final stage of electrolysis. When the electrolysis time reached 18 h, the decomposition rate of ammonium sulfate was 96.15%. The decomposition rates measured in the subsequent 12 h varied between 96.11% and 96.20%. At the beginning of electrolysis, under the action of a direct current electric field, ions in the middle compartment moved to the compartments on both sides through the membranes. With the decreasing ammonium sulfate concentration in the middle compartment, in the final stage of electrolysis, the number of ions entering the compartments on both sides was similar to the number of ions diffusing back to the middle compartment, which maintained the decomposition rate about 96.15%. In addition, the cell voltage dropped from 21 V to 10.9 V within 2 h after the start of electrolysis, then slowly declined and stabilized between 8.1 V and 8.5 V. It was found that the cell voltage slowly rose to 9 V within the last 4 h of electrolysis. The reason may be that when electrolysis is initiated, the ammonia concentration in the cathode compartment is relatively low and, as a result, the conductivity is quite poor and the resistance of the entire system

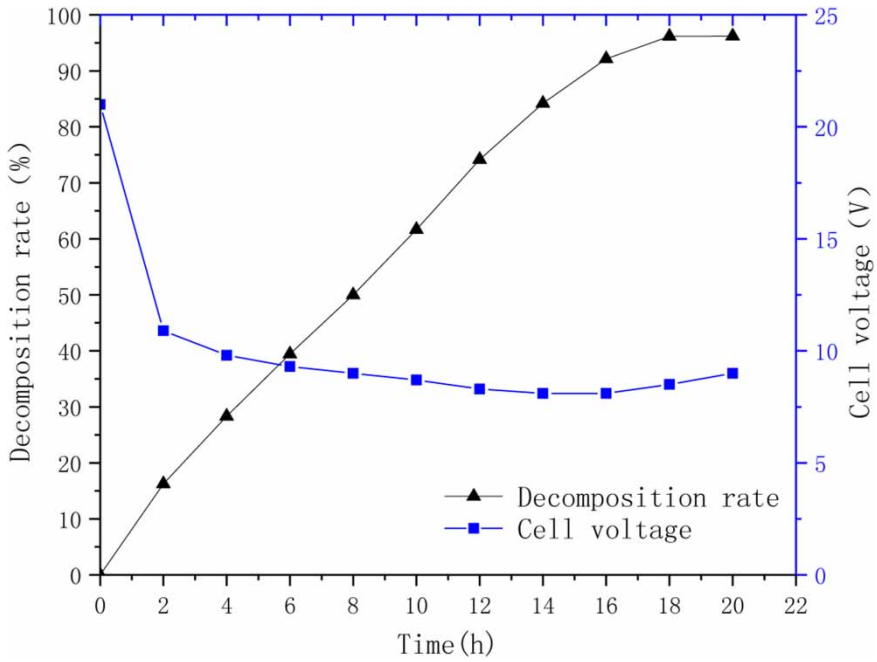

Figure 6 | Decomposition rate and cell voltage versus time (current density 250 A/m^2, T = 40 °C, 0.05 mol/L H_2SO_4, 0.05 mol/L $NH_3{\cdot}H_2O$).

and voltage are too high. As the electrolysis reaction progresses, the concentration of ammonia increases and the system voltage gradually decreases. After 18 h, the concentration of ammonium sulfate decreased, its decomposition became slower, and the resistance of the middle compartment increased while the cell voltage increased slightly. The acid and base concentrations in the compartments on both sides changed with time, as shown in Figure 7. The

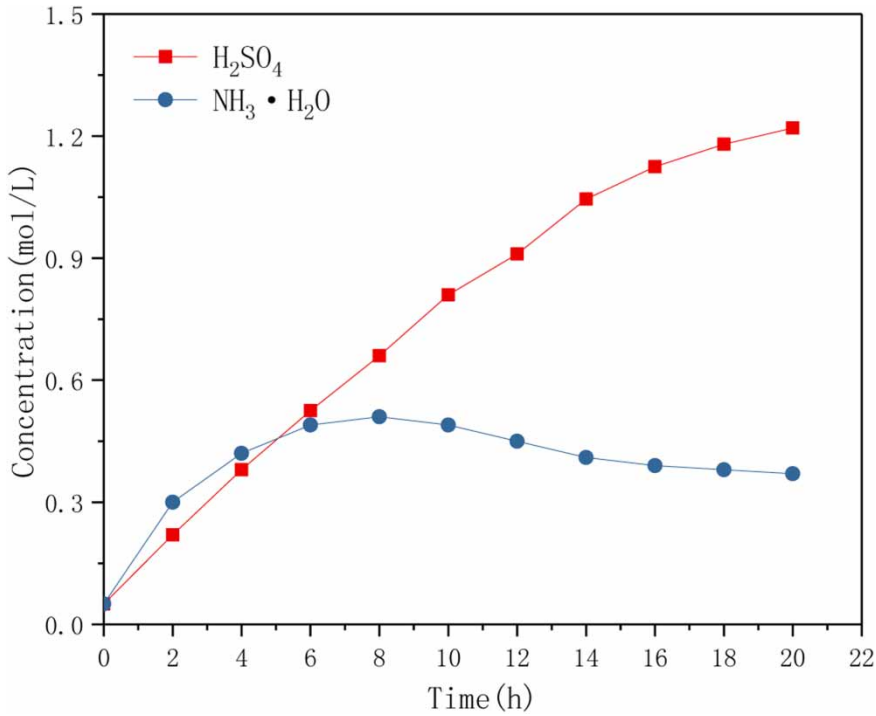

Figure 7 | Variations in the acid and base concentrations in both compartments over time (current density 250 A/m^2, T = 40 °C, 0.05 mol/L H_2SO_4, 0.05 mol/L $NH_3{\cdot}H_2O$).

concentration of sulfuric acid increased at the beginning of electrolysis. As the concentration of ammonium sulfate in the middle compartment decreased, the growth rate slowed down. The stirring action of the gas continuously promoted the evaporation of ammonia, and it was impossible to obtain a high concentration of ammonia in the cathode chamber. As the sulfuric acid concentration in the anode chamber increased continuously, H^+ leaked into the middle compartment and then entered the cathode chamber through the anode membrane to react with ammonia. Therefore, the ammonia concentration decreased slowly. To prevent ammonia from overflowing and polluting the atmosphere and to fully recover ammonia in actual production, an ammonia absorption process can be implemented at the end.

Analysis and discussion of substances produced by removal of impurities

Excess ammonium bicarbonate was added in the two-step impurity removal process, in which HCO_3^- was passed through the anion exchange membrane to reach the anode chamber where it reacted with H^+ in the anode chamber to generate carbon dioxide and water. No new impurities were introduced into the system. XRD analysis of the substance obtained by filtration after adding ammonium bicarbonate to the solution when Mn^{2+} is removed in the first step is shown in Figure 8. The characteristic peaks correspond to the characteristic peaks of manganese carbonate at the bottom of Figure 8, and the manganese carbonate obtained in this manner is high grade and can be directly used in the ore leaching process of electrolytic manganese production. XRD analysis of the substance obtained after adding ammonium bicarbonate to the solution except Mg^{2+} in the second step is shown in Figure 9. A slight right shift of the characteristic peaks of magnesium carbonate was observed, which may be attributed to a small amount of the ASDSC precipitate formed because of the temperature reduction in the filtration process. Magnesium carbonate can be used to produce pipeline insulation materials in factories, and a small amount of impurities are acceptable. Sulfuric acid and ammonia water produced by electrolysis can also be directly recycled to the different stages of electrolytic manganese production.

CONCLUSIONS

The double-membrane three-chamber electrolysis method is a new strategy to address the issue of ASDSCs formed during the electrolytic production of manganese. The pretreated manganese carbonate can be reused in the production of electrolytic manganese, and magnesium carbonate can be used to make fireproof insulation materials.

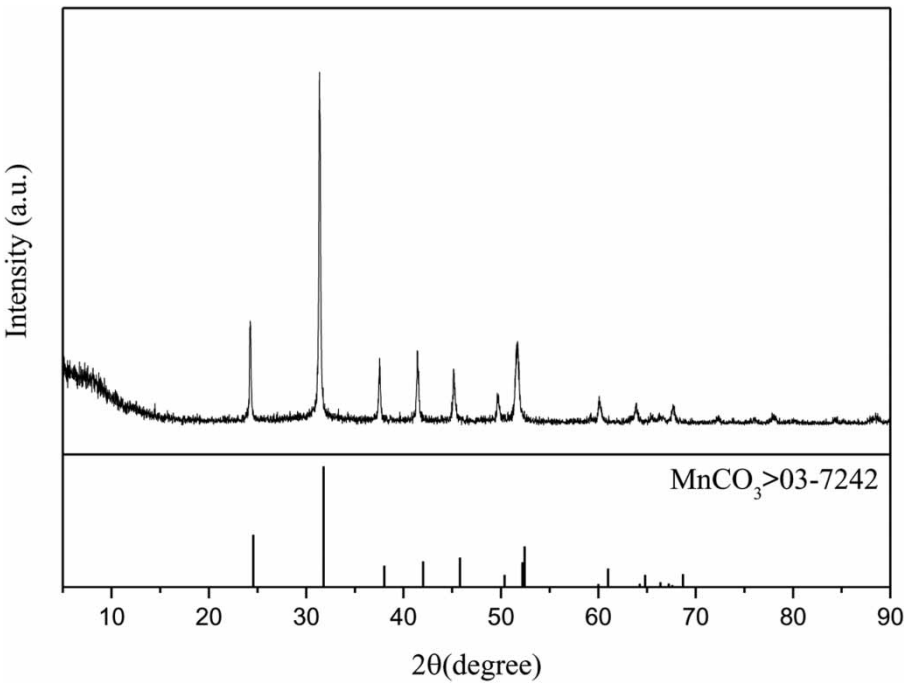

Figure 8 | XRD analysis of the first filtered product.

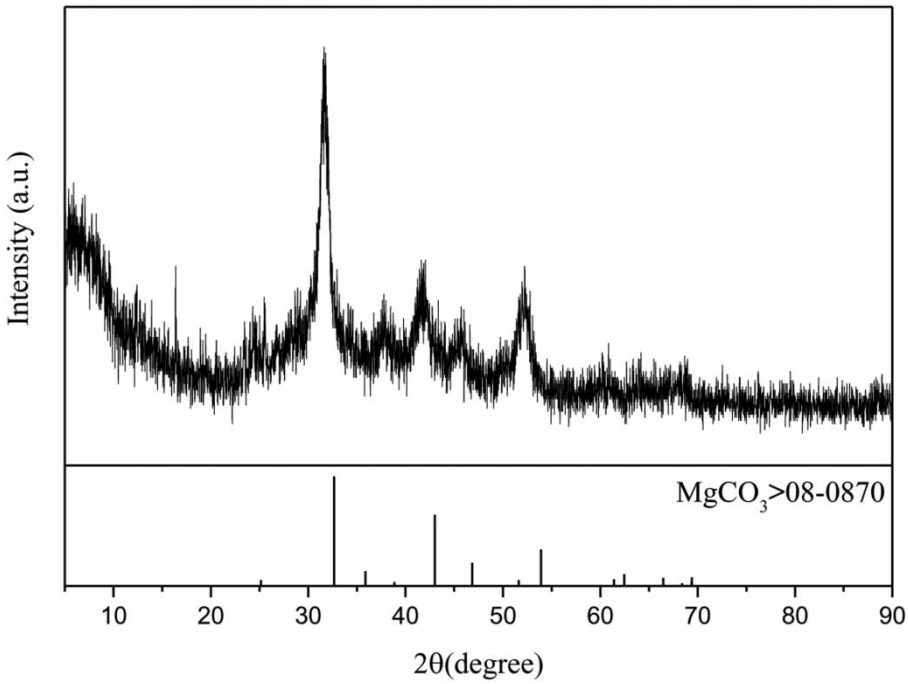

Figure 9 | XRD analysis of the second filtered product.

Experiments show that the decomposition rate of ammonium sulfate reached 96.15% under the conditions of AMV and Nafion-117 membrane, current density of 250 A/m^2, T = 40 °C, and decomposition time of 18 h. The complete treatment process makes full use of ASDSCs and is environmentally friendly. However, as the construction cost of the membrane module in this process is relatively high, the focus of future research is to reduce the treatment cost. In actual production, the electrode plate area can be increased and its spacing can be reduced, the cell voltage can be reduced, and multiple groups of electrolytic cells can be connected in parallel to make full use of the electrode plate area, reduce energy consumption, and gain further economic benefits.

ACKNOWLEDGEMENTS

This project was supported by the National Natural Science Foundation of China (No. 21466019).

DATA AVAILABILITY STATEMENT

All relevant data are included in the paper or its Supplementary Information.

REFERENCES

Cheng, Y. W., Ding, F. Q. & Fei, Y. 2010 Slurry electrolysis of ocean polymetallic nodule. *Transactions of Nonferrous Metals Society of China* **20**, 60–64.

Feng, Y., Chen, Y. X., Liu, F. & Bao, X. 2006 Study on the production of cement retarder by electrolytic manganese slag. *Modern Chemicals* **26** (2), 57–60.

Jia, T. J., Zhang, Z. H., Duan, F., Song, Z. P., Liu, N., Tian, Z., Zhang, B. & Zhou, J. 2018 A treatment method of double salt crystal in the process of electrolytic manganese. CN108396158A[P], China.

He, S. C., Liu, Z. H., Liu, Z. Y., Xia, L. G., Ma, H. & Zhu, Y. 2011 Comprehensive utilization method of electrolytic manganese anode slag and electrolytic manganese crystal double salt. CN108842052A[P], China.

Li, H., Zhang, Z., Tang, S., Li, Y. & Zhang, Y. 2008 Ultrasonically assisted acid extraction of manganese from slag. *Ultrasonics Sonochemistry* **15** (4), 339–343.

Li, C., Zhong, H., Wang, S., Xue, J. & Zhang, Z. 2015a A novel conversion process for waste residue: synthesis of zeolite from electrolytic manganese residue and its application to the removal of heavy metals. *Colloids and Surfaces A: Physicochemical and Engineering Aspects* **470**, 258–267.

Li, C., Zhong, H., Wang, S., Xue, J. & Zhang, Z. 2015b Removal of basic dye (methylene blue) from aqueous solution using zeolite synthesized from electrolytic manganese residue. *Journal of Industrial and Engineering Chemistry* **23**, 344–352.

Lu, J., Dreisinger, D. & Glück, T. 2014 Manganese electrodeposition – A literature review. *Hydrometallurgy* **141**, 105–116.

Luo, T., Abdu, S. & Wessling, M. 2018 Selectivity of ion exchange membranes: a review. *Journal of Membrane Science* **555** (1), 429–454.

Park, J. S., Choi, J. H., Woo, J. J. & Moon, S. 2006 An electrical impedance spectroscopic (EIS) study on transport characteristics of ion-exchange membrane systems. *Journal of Colloid and Interface Science* **300**, 655–662.

Sata, T. 2000 Studies on anion exchange membranes having permselectivity for specific anions in electrodialysis – effect of hydrophilicity of anion exchange membranes on permselectivity of anions. *Journal of Membrane Science* **167** (1), 1–31.

Shi, Y., Jiang, K., Zhang, T. & Lv, G. 2019 Cleaner alumina production from coal fly ash: membrane electrolysis designed for sulfuric acid leachate. *Journal of Cleaner Production*. https://doi.org/10.1016/j.jclepro.2019.118470.

Shu, J. C., Liu, R. L., Liu, Z., Chen, H. & Tao, C. 2016a Enhanced extraction of manganese from electrolytic manganese residue by electrochemical. *Journal of Electroanalytical Chemistry* **780**, 32–37.

Shu, J., Liu, R., Liu, Z., Chen, H., Du, J. & Tao, C. 2016b Solidification/stabilization of electrolytic manganese residue using phosphate resource and low-grade MgO/CaO. *Journal of Hazardous Materials* **317**, 267–274.

Shu, J., Wu, H., Liu, R., Liu, Z., Li, B., Chen, M. & Tao, C. 2018 Simultaneous stabilization/solidification of Mn^{2+}, and NH_4^+-N from electrolytic manganese residue using MgO and different phosphate resource. *Ecotoxicology and Environmental Safety* **148**, 220–227.

Tanaka, Y. 2003 Mass transport and energy consumption in ion-exchange membrane electrodialysis of seawater. *Journal of Membrane Science* **215** (1), 265–279.

Tao, C. Y., Sun, S. & Liu, R. L. 2011 Method for Recovering manganese and magnesium from complex salt crystals produced by electrolytic manganese process. CN102154556A[P], China.

Wang, Q. N., Wang, K., Liu, B., Gao, X. & Xu, D. 2012 Analysis and control of ammonia nitrogen pollution in electrolytic manganese industry in China. *Environmental Engineering* **30** (3), 121–123.

Yang, C., Lv, X., Tian, X., Wang, Y. & Komarneni, S. 2014 An investigation on the use of electrolytic manganese residue as filler in sulfur concrete. *Construction and Building Materials* **73**, 305–310.

Ye, F., Cheng, H., Xu, L., Hu, S., Li, B., Shi, W. & Leng, S. 2018 Study on preparation of light porous ceramic block material from electrolytic manganese slag. *Inorganic Salt Industry* **50** (10), 62–65.

Zhang, H., Bi, Y., Chen, X., Huang, L. & Mu, L. 2016 Treatment and characterization analysis of electrolytic manganese anode slime. *Procedia Environmental Sciences* **31**, 683–690.

Zhang, W. J., Ma, J., Wang, Z. W. & Liu, H. L. 2017 Investigations on electrochemical properties in mass transport of ion exchange membrane. *Membrane Science and Technology* **37**, 44–50.

Zhou, L. X. 2010 Review and prospect of China's electrolytic manganese industry for more than 50 years. *China's Manganese Industry* **28** (1), 1–6.

Zhou, C., Wang, J. & Wang, N. 2013 Treating electrolytic manganese residue with alkaline additives for stabilizing manganese and removing ammonia. *Korean Journal of Chemical Engineering* **30** (11), 2037–2042.

Zhou, C., Du, B., Wang, N. & Chen, Z. 2014 Preparation and strength property of autoclaved bricks from electrolytic manganese residue. *Journal of Cleaner Production* **84**, 707–714.

Zhou, J., Wang, S. F. & Song, X. 2016 Electrodeposition of cobalt in double-membrane three-compartment electrolytic reactor. *Transactions of Nonferrous Metals Society of China* **26** (06), 1706–1713.

First received 27 February 2020; accepted in revised form 24 July 2020. Available online 10 August 2020